JOURNAL OF SOLID STATE CHEMISTRY **141,** 1–9 (1998)
ARTICLE NO. SC987850

Synthesis, Structure, and Magnetic Properties of $Sr_{39}Co_{12}N_{31}$

Glen R. Kowach,[1] H. Y. Lin,[2] and F. J. DiSalvo[3]

Baker Laboratory, Department of Chemistry, Cornell University, Ithaca, New York 14853

Received November 17, 1997; in revised form April 6, 1998; accepted April 15, 1998

Single crystals of $Sr_{39}Co_{12}N_{31}$ have been synthesized in liquid sodium from strontium, cobalt, and sodium azide at 1000°C in sealed niobium ampoules. The structure was solved by single-crystal X-ray diffraction ($Im\bar{3}m$ (No. 229), $a = 14.910$ Å, $Z = 2$, $R(F) = 6.7\%$, $R_w(F) = 6.3\%$) with a disordered strontium position. $Sr_{39}Co_{12}N_{31}$ has a unique structure type incorporating cobalt in linear coordination as isolated nitridometalate ions. All cobalt atoms are crystallographically equivalent, existing with a formal mixed valence of Co^{I} and Co^{II}. The magnetic susceptibility demonstrates antiferromagnetic Curie–Weiss behavior with an effective moment on cobalt of 4.99 μ_B, which lies in the range expected for that of high-spin ground states.

INTRODUCTION

Solid-state nitrides are of great interest for their unusual structures (1), high thermal conductivity (AlN)) (2), high specific modulus (Si_3N_4) (3), resilient mechanical strength and hardness (TiN) (4), emission of blue light (GaN) (5), and superconducting (NbN) (6) properties. Recently, we have focused on ternary late transition metal nitrides to study the unusual low coordination of the transition metal by nitrogen. Linear anions are a common motif in ternary late transition metal nitrides. Metals with two collinear bonds are present in the following structures as isolated anions or one-dimensional chains: (*a*) substitutionally disordered or defect variants of the lithium nitride structure ($Li_2[(Li_{1-3x}Fe_x)N]$ (7), $Li_2[(Li_{1-x}Fe_x)N]$ (7), $Li_2[(Li_{1-x}Co_x)N]$ (8), $Li_2[(Li_{1-x}Ni_x)N]$ (9), $Li_2[(Li_{1-x}Cu_x)N]$ (8), Li_4FeN_2 (10), $Ba_2(Ni_{1-x}Li_x)[NiN]_2$ (11)), (*b*) structures related to Li_4SrN_2, which contain fragments of the Li_3N type ($Li_2Sr[(Li_{1-x}Cu_x)N]_2$ (12), $(Li_{1-x}Ni_x)Li_3SrN_2$ (13)), (*c*) those similar to the α-Li_3BN_2 type ($LiSr_2CoN_2$ (14), $Ca_2(Li_{1-x}Cu_x)[(Li_{1-x}Cu_x)N_2]$ (12)), (*d*) the YCoC structure (CaNiN (15), $Ca(Li_{1-x}Ni_x)N$ (16), $(Ca_{1-x}Sr_x)NiN$ (17)) or structures containing a fragment of YCoC ($(Li_{1-x}Ni_x)Li_4Sr_2N_3$ (18)), (*e*) BaNiN type (BaNiN (19), SrNiN (17), $Sr[(Li_{1-x}Ni_x)N]$ (18), $Sr[(Li_{1-x}Cu_x)N]$ (12), SrCuN (20)), and structures with similarities to the BaNiN structure (BaCoN (21)), (*f*) the delafossite structure ($CuTaN_2$ (22)), and (*g*) other structures such as FeNiN (23), Sr_2FeN_2 (24), $Ba_8Ni_6N_7$ (25), $Li_3Sr_3Ni_4N_4$ (26), Sr_2NiN_2 (27), $Sr_6Cu_3N_5$ (28), and A_2ZnN_2 (A = Ca (29), Sr, Ba (30)). In the substitutionally disordered phases, infinite one-dimensional MN chains are formed with probabilistic transition metal and lithium occupation of the M site.

The few previously known cobalt nitride ternary compounds are the following: Ca_3CoN_3 with Co^{III} in trigonal-planar coordination (31), BaCoN with Co^{I} in linear coordination forming one-dimensional zigzag chains (21), and $Li_2[Li_{1-x}Co_x)N]$ (8) and $LiSr_2CoN_2$ (14) with Co^{I} in linear coordination. Although most ternary nickel nitrides form Ni^{I} species, we have recently discovered the formation of Ni^{II} in Sr_2NiN_2 (27). On the basis of this knowledge, we searched for ternary cobalt nitrides with unusual oxidation states by the liquid sodium flux technique. In this paper, the synthesis, structure, and magnetic properties of $Sr_{39}Co_{12}N_{31}$, the first example of a formally mixed-valent cubic ternary cobalt nitride, are discussed.

EXPERIMENTAL

Preparation of $Sr_{39}Co_{12}N_{31}$

All manipulations were carried out in helium or argon atmospheres due to the high moisture sensitivity of the reactants and products. Crystals of $Sr_{39}Co_{12}N_{31}$ were synthesized in welded niobium ampoules (seamless tubing, o.d. 3/8 in., wall thickness 0.020 in., length approximately 4 in., minimum 99.9%, Specialty Steel and Forge, etched before use with a concentrated acidic solution containing 15% HF, 40% H_2SO_4, and 45% HNO_3 by volume). A mixture of strontium (rod, 98%, Strem), cobalt powder (− 325 mesh, 99.8%, Johnson Matthey, purified in a H_2 atmosphere), NaN_3 (99%, Aldrich), and sodium (lump, 99%, Aldrich) was added such that the nominal molar ratio of elements was

[1]Current address: Bell Laboratories, Lucent Technologies, 700 Mountain Avenue, Murray Hill, NJ 07974.

[2]Current address: Noyes Laboratory, Department of Chemistry, University of Illinois, Urbana, IL 61801.

[3]To whom correspondence should be addressed.

0022-4596/98 $25.00

approximately 2 Sr:2 Co:3 N:6 Na (0.1601 g of Sr, 0.1088 g of Co, 0.0609 g of NaN_3, 0.1052 g of Na). The ampoule was sealed in an evacuated fused-silica tube, heated to 1000°C for 96 h, and slowly cooled to 500°C over an additional 96 h. Crystals were isolated from the sodium flux by washing with liquid ammonia. The high solubility of sodium in liquid ammonia and negligible reactivity of the nitrides at the extraction temperature allowed for the separation of crystals from the flux. A glass apparatus, which has been previously described, was employed for the extraction (32). Ammonia, purified by sodium metal to remove any water contamination, was condensed onto the reaction products by applying a dry ice/2-propanol bath. The sodium solution was then filtered through a glass frit, and the ammonia evaporated. There was no evidence of attack of the niobium container by the sodium flux or the reactants. The product was a mixed phase containing clusters of black $Sr_{39}Co_{12}N_{31}$ crystals having a habit that is slightly distorted from isometric (Fig. 1) (33), large hexagonal platy crystals of Sr_2N, and cobalt metal. The Sr_2N crystals were identified by unit cell parameters ($R\bar{3}m$: $a = 3.849$ Å and $c = 20.612$ Å) from single-crystal X-ray diffraction (34), and the excess cobalt was observed due to its ferromagnetic behavior. Relatively pure $Sr_{39}Co_{12}N_{31}$ was obtained by physically separating the Sr_2N crystals and collecting the excess cobalt with a magnet. The yield of $Sr_{39}Co_{12}N_{31}$ was approximately 15% based on strontium as the limiting reagent. Single crystals examined by a windowless microprobe indicated no sodium or niobium contamination with error $<1\%$ (35). Elemental analysis was performed on a 20 mg sample at Galbraith Laboratories by using inductively coupled plasma (ICP) spectrographic analysis. The following weight percentages were determined. Calcd. for $Sr_{39}Co_{12}N_{31}$: Sr, 74.95; Co, 15.53; N, 9.52. Found (% error): Sr, 72.93 (3.70); Co, 14.51 (0.84); N, 12.56 (N by difference). The atomic ratio of the metals was found to be 39 Sr:11.54 Co, which is in excellent agreement with the crystallographic analysis. The strontium content may be slightly high due to small crystals of Sr_2N which could not be easily separated. The nitrogen stoichiometry for $Sr_{39}Co_{12}N_{31}$ is derived from X-ray diffraction data, and therefore, potential oxygen impurities were not explicitly measured. Since the nitrogen content by ICP is determined by difference, any impurities in the sample (including decomposition due to exposure to air) are included in this value.

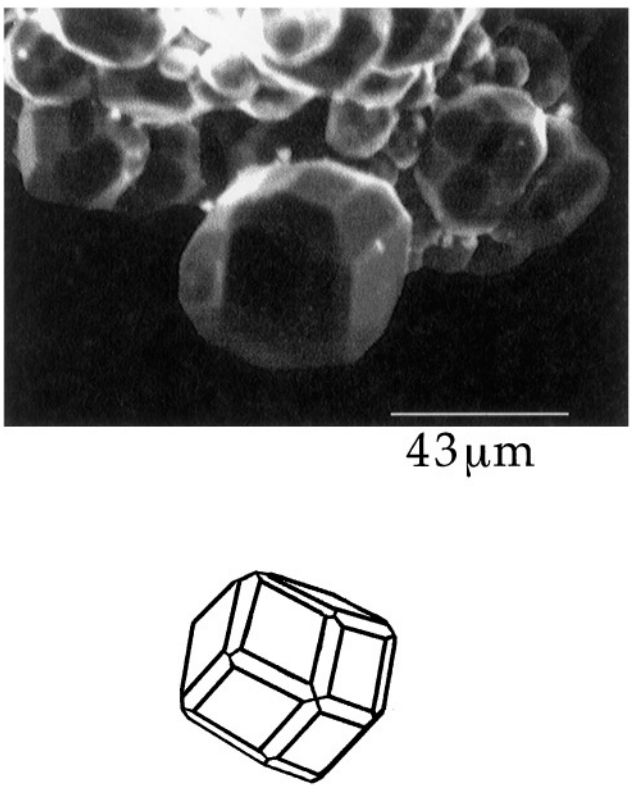

FIG. 1. A scanning electron micrograph of a cluster of crystals of $Sr_{39}Co_{12}N_{31}$ shows a slight distortion from isometric habit. The ideal habit can be described as a dodecahedron (bound by the [110] faces) with edges truncated by a trapezohedron (bound by the [211] faces), which is similar to the habit of garnets.

X-Ray Diffraction Data

A single crystal of $Sr_{39}Co_{12}N_{31}$ was sealed in a thin walled glass capillary. The intensity data were collected on a Rigaku AFC7R diffractometer with graphite-monochromated Mo$K\alpha$ ($\lambda = 0.71069$ Å) radiation generated from a rotating anode at 50 kV and 250 mA power settings. Crystallographic data are summarized in Tables 1–5.

Cell constants, which were obtained from 24 centered reflections in the range $21^\circ < 2\theta < 29^\circ$, indicate a cubic unit cell. The Laue checks for cubic symmetry ($hkl \rightarrow klh$, 3-fold axis, R merge = 2.4%; $hkl \rightarrow k\text{-}hl$, 4-fold axis parallel to c, R merge = 2.6%) were passed by comparing the above symmetry-equivalent reflections of 23 general reflections of the 24 centered reflections. This uniquely identifies the Laue class to be $4\bar{3}m$. Data were collected in the $(+h, +k, +l)$ octant; all reflections were collected. Based on systematic absences (hkl: $h + k + l \neq 2n$), which reveal a body-centering condition, the centrosymmetric space group was uniquely determined to be $Im\bar{3}m$ (No. 229). Although the final structure is disordered (vide infra), the $Im\bar{3}m$ space group was determined by the Laue class. There is no evidence of ordering by X-ray diffraction.

The data were collected at room temperature using the ω–2θ scan technique in the 2θ range 5.4–60.0°. Of the 1031 reflections that were collected, all were unique for refinement purposes. The intensities of the standard reflections were collected every 150 reflections, and there was no observable decay. No absorption correction was applied to the data due to the spherical shape of the crystal. Empirical

TABLE 1
Crystallographic Information for $Sr_{39}Co_{12}N_{31}$

Empirical formula	$Sr_{39}Co_{12}N_{31}$
Formula weight	4558.59 g/mol
Diffractometer type	Rigaku AFC7R
Monochromator	Graphite
Scan type	ω–2θ
Temperature	291(3) K
Wavelength	Mo$K\alpha$
Crystal system	Cubic
Space group	$Im\bar{3}m$ (No. 229)
Unit cell parameter	$a = 14.910(5)$ Å
Volume	3314.4(5) Å^3
Z	2
Density (calculated)	4.57 g/cm^3
Absorption coefficient	339.6 cm^{-1}
$F(000)$	4046
Crystal size	Roughly 50-μm-diameter sphere
Crystal color	Black
2θ range	$5.4^\circ < 2\theta < 60.0^\circ$
Reflections collected	1031
Independent reflections	516
Refinement method	Direct methods (SAPI90)
Extinction coefficient	7.2403×10^{-9}
Data/parameters	243/29
Goodness-of-fit	2.11
Maximum shift/error	0.0009
Final R indices $[I > 2\sigma(I)]^a$	$R(F) = 6.7\%$, $R_w(F) = 6.3\%$
Maximum peak in diffraction map	3.37 e/Å^3
Minimum peak in diffraction map	-4.92 e/Å^3

$^a R(F) = \sum\|F_o| - |F_c\|/\sum|F_o|$ and $R_w(F) = \sum[w\|F_o| - |F_c\|^2/\sum w|F_o|^2]^{1/2}$ where $w = 1/\sigma^2$.

ψ-scan absorption data were collected and displayed minimum and maximum normalized transmission factors ranging from 0.90 to 1.00. However, application of a ψ-scan absorption correction did not decrease the residuals. The data were corrected for Lorentz–polarization effects.

TABLE 2
Atomic Coordinates and Equivalent Isotropic Displacement Parameters

Atom	Site	x	y	z	$B_{eq}{}^a$ (Å^2)	Occupancy
Sr1	48k	0.4669(5)	0.3354(7)	0.4669	1.21(11)	0.25
Sr2	48k	0.3772(1)	0.1857(2)	0.3772	1.60(4)	1
Sr3	12d	$\frac{1}{4}$	0	$\frac{1}{2}$	0.57(6)	1
Sr4	6b	0	$\frac{1}{2}$	$\frac{1}{2}$	0.73(10)	1
Co1	24h	0	0.2879(2)	0.2879	0.80(6)	1
N1	24h	0	0.201(1)	0.201	0.7(6)	1
N2	24h	0	0.373(2)	0.373	1.8(7)	1
N3	12e	0.328(3)	0	0	0.2(7)	1
N4	2a	0	0	0	0.6(11)	1

$^a B_{eq} = 8/3\,\pi^2(U_{11}(aa^*)^2 + U_{22}(bb^*)^2 + U_{33}(cc^*)^2 + 2U_{12}aa^*bb^*\cos\gamma + 2U_{13}aa^*cc^*\cos\beta + 2U_{23}bb^*cc^*\cos\alpha)$.

TABLE 3
Anisotropic Displacement Parameters

Atom	U_{11}	U_{22}	U_{33}	U_{12}	U_{13}	U_{23}
Sr1	0.020(3)	0.005(5)	0.020	0.001(3)	0.002(4)	0.001
Sr2	0.0155(9)	0.030(2)	0.0155	0.006(1)	0.009(1)	0.006
Sr3	0.005(3)	0.008(2)	0.008	0.0000	0.0000	0.0000
Sr4	0.008(5)	0.010(3)	0.010	0.0000	0.0000	0.0000
Co1	0.017(3)	0.007(2)	0.007	0.002(2)	0.0000	0.0000

Note: The anisotropic displacement factor expression is as follows: $\exp(-2\pi^2(a^{*2}U_{11}h^2 + b^{*2}U_{22}k^2 + c^{*2}U_{33}l^2 + 2a^*b^*U_{12}hk + 2a^*c^*U_{13}hl + 2b^*c^*U_{23}kl))$.

The structure was solved by direct methods (SAPI90) (36) followed by least-squares refinement in the teXsan software package (37). All heavy atoms were refined anisotropically. The final cycle of the full-matrix least-squares refinement based on F was performed on 243 observed reflections ($I > 2\sigma(I)$) with 29 variables leading to a data to parameter ratio of 8.38 : 1. The residuals after the final cycle were $R(F) = 6.7\%$ and $R_w(F) = 6.3\%$, with the maximum and minimum peaks in the difference Fourier map of 3.37 and -4.92 e/Å^3, respectively. One strontium atom, Sr1, was refined at (x, x, z). This position is slightly off the higher symmetry position (x, 0, 0) on the cell edge, thereby generating four equivalent positions. The positions were split by 0.99(1) Å and refined each with $\frac{1}{4}$ occupancy. An ORTEP plot of the asymmetric unit is presented in Fig. 2.

TABLE 4
Selected Interatomic Distances (Å)[a]

Co1–N1	1.84(3)	Sr2–N2	2.770(3)
Co1–N2	1.79(4)	Sr2–N3	2.596(4)
Sr1–N1	2.60(3)	Sr2–Sr1	2.93(1)
Sr1–N3	2.53(4)	Sr2–Sr1	3.489(7)
Sr1–N4	2.55(1)	Sr2–Sr1	3.97(1)
Sr1–Sr1	2.77(2)	Sr2–Sr1	4.445(9)
Sr1–Sr1	0.99(1)	Sr2–Sr2	4.039(5)
Sr1–Sr1	2.94(1)	Sr2–Sr2	4.019(5)
Sr1–Sr1	3.54(1)	Sr2–Sr2	3.661(4)
Sr1–Sr1	3.68(1)	Sr2–Sr4	3.790(3)
Sr1–Sr1	2.94(1)	Sr3–Co1	3.213(3)
Sr1–Sr1	1.40(2)	Sr3–N2	2.6361(7)
Sr1–Sr1	4.17(2)	Sr3–Sr2	3.822(2)
Sr1–Sr1	4.28(2)	Sr3–Sr4	3.727(1)
Sr2–Co1	3.093(3)	Sr4–N2	2.68(4)
Sr2–Co1	3.348(4)	Sr4–N3	2.57(4)
Sr2–N1	2.752(4)		

[a]Includes symmetry-equivalent positions.

TABLE 5
Selected Bond Angles (deg)

Linear CoN_2 anion	
N2–Co1–N1	180
Disordered Sr_6N octahedra centered about (0, 0, 0)[a]	
Sr1a–N4–Sr1b	22.3(3)
Sr1a–N4–Sr1c	31.7(4)
Sr1a–N4–Sr1e	87.86(6)
Sr1a–N4–Sr1f	92.14(6)
Sr1a–N4–Sr1g	70.5(2)
Sr1a–N4–Sr1h	65.8(4)
Sr1a–N4–Sr1a′	180
Sr1a–N4–Sr1b′	157.7(3)
Sr1a–N4–Sr1c′	148.3(4)
Sr1a–N3–Sr1b	21.9(4)
Sr1a–N3–Sr1g	68.9(9)
Sr1a–N3–Sr1h	64.4(8)
Sr_5CoN octahedra centered about N2	
Sr2–N2–Sr2	176(1)
Sr2–N2–Sr3	89.97(4)
Sr2–N2–Sr4	88.1(7)
Sr3–N2–Sr3	178(1)
Sr3–N2–Sr4	89.0(8)
Co1–N2–Sr2	91.9(7)
Co1–N2–Sr3	91.0(8)
Co1–N2–Sr4	180
Sr_6CoN capped triangular prism about N1[b]	
Sr2a–N1–Sr2b	83.4(2)
Sr2a–N1–Sr2d	94.4(2)
Sr2a–N1–Sr2c	164(1)
Sr2a–N1–Sr1a	72.1
Sr2a–N1–Sr1b	122.0
Co1–N1–Sr2a	82.1(6)
Co1–N1–Sr1a	145.1
Sr2a–Sr1a–Sr2b	64.8
Sr1a–Sr2b–Sr2a	57.6
Sr2a–Co1–Sr2b	72.6(1)
Sr2a–Co1–Sr2c	123.6(2)
Sr2a–Co1–Sr2d	81.5(1)

[a]See Fig. 7 for label assignments.
[b]Sr1 is at ($\frac{1}{2}$, 0.3354, $\frac{1}{2}$) for clarity. See Fig. 4 for label assignments.

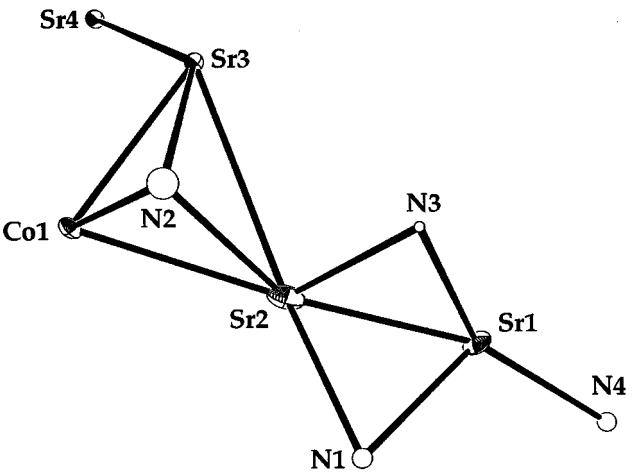

FIG. 2. ORTEP plot of the asymmetric unit of $Sr_{39}Co_{12}N_{31}$ drawn at the 50% probability level. All anisotropic thermal elipsoids for the heavy atoms demonstrate reasonable displacements. The isotropic thermal parameters vary significantly for the nitrogen atoms. However, the structure solution restrained to equal nitrogen parameters refined to $B_{eq} = 1.0(3)$ Å^2 without noticeable change in the residuals.

Magnetic Susceptibility

The magnetic susceptibility data were collected on a SQUID magnetometer (Quantum Design MPMS System). A 25-mg sample was placed into a gelatin capsule in a helium-filled glove box and mounted in a plastic straw. Most of the ferromagnetic cobalt metal impurity was removed from the product by passing a magnet over the sample. The sample was cooled to 200 K and centered until a symmetric signal was obtained. The field-dependent data indicated a small ferromagnetic impurity. Temperature-dependent data were collected from 5 to 300 K in 2 K steps with an applied field of 10,000 Oe. Upon thermal cycling, the sample decomposed when reheated from 5 K to temperatures above 275 K, leading to the formation of an additional ferromagnetic impurity, perhaps cobalt metal. It seems unlikely that thermal cycling alone would decompose the sample because $Sr_{39}Co_{12}N_{31}$ is stable at room temperature for several months. Therefore, the decomposition may be due to a possible moisture contamination.

RESULTS AND DISCUSSION

Sodium Flux Crystal Growth

Recently, sodium–alkaline earth fluxes have proved useful in the synthesis of nitrides. Several ternary nitrides containing alkaline earth and transition metals have been synthesized by this technique: Sr_2NiN_2 (27), BaNiN (38), SrCuN (28), $Sr_6Cu_3N_5$ (28), Sr_2ZnN_2, and Ba_2ZnN_2 (30). Due to high alkaline earth metal to transition metal ratios, the products are often composed mainly of isolated transition metal nitride anions. Previously, Jacobs *et al.* found that $NaNH_2$ decomposes at moderate temperatures into nitrogen and hydrogen gases and molten sodium, which then acts as a flux to grow single crystals of early transition metal ternary nitrides (39).

To rationalize the crystallization process in a sodium flux, it is necessary to examine the solubilities of the elements in the melt and determine possible dissolution species. Nitrogen is virtually insoluble in pure liquid sodium (10^{-10} wt% in pure sodium at 600°C) (40). However, in a melt containing sodium and even a few mole percent of an alkaline earth

metal, the solubility of nitrogen is increased to approximately 1 mol% (41, 42). Addison *et al.* suggested that a Ba_4N cluster is the dissolution species based on precipitation studies in the Na–Ba–N system (43). However, crystallographic information provided by Simon *et al.* on subnitrides in the sodium–alkaline earth system indicates that the most probable dissolution species is a nitrogen-centered, A_6N, octahedral species, where A = Ca, Sr, and Ba (44–48). The solubility of cobalt in pure liquid sodium at 1000°C is less than 5 ppm for cobalt (49). This would appear to be the limiting solubility factor in the sodium flux; however, even a slight impurity of oxygen increases the solubility significantly (50). Dissolved nitrogen, by extension of this concept, may increase the solubility of transition metals by the formation of soluble transition metal–nitrogen complexes. With this information, it may be possible to design synthetic mechanisms for the formation of late transition metal ternary nitrides.

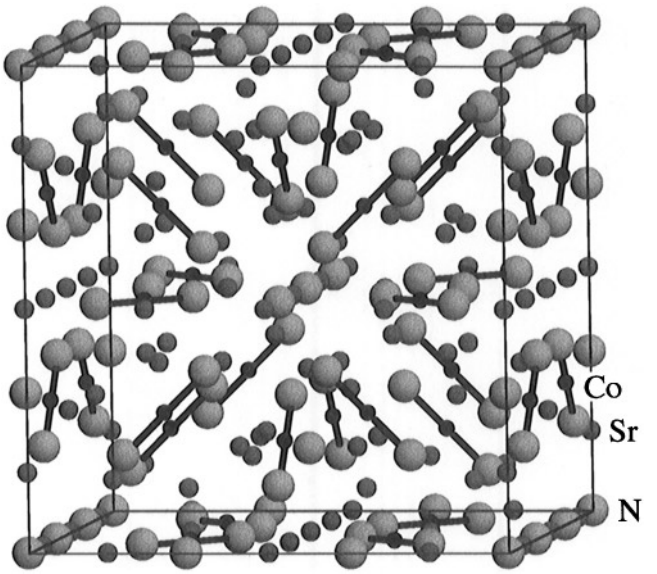

FIG. 3. The Body-centered cubic unit cell illustrated for $Sr_{39}Co_{12}N_{31}$. Strontium, cobalt, and nitrogen atoms are represented by dark gray, black, and light gray spheres of arbitrary size, respectively. The bonding in the linear CoN_2 anions is highlighted. The disordered strontium position, Sr1, is placed in the high-symmetry position on the cell edge for clarity.

Synthetic Variations

Crystals of $Sr_{39}Co_{12}N_{31}$ were grown by using either strontium metal or strontium nitride as a starting material. The conditions for optimal yield were found using strontium metal as described in the experimental section. Substitution of Sr and NaN_3 with strontium nitride, "Sr_3N_2," also yields $Sr_{39}Co_{12}N_{31}$, but in significantly smaller quantities. Experiments with strontium at 900°C resulted in small yields, whereas experiments at 1000°C with a slow cool and those quenched from 1000°C demonstrated similar yields around 15%. Reaction conditions based on $Sr_{39}Co_{12}N_{31}$ initial stoichiometric amounts do not improve yield. The foregoing yield comparisons are estimated from powder X-ray diffraction data.

Structural Description

The first example of a ternary nitride in the Sr–Co–N system, $Sr_{39}Co_{12}N_{31}$, has a unique structure type based on body-centered cubic symmetry. The unit cell contains 164 atoms, leading to a complex structure. The prominent structural features include isolated linearly coordinated CoN_2 anions, an interpenetrating, vertex-sharing, octahedral Sr–N subframework, and a disordered strontium position.

In the planes that include the faces of the unit cell, four CoN_2 ions point toward the center of the face such that two of the ions lie on each face diagonal (Fig. 3). In addition, there are four CoN_2 ions that lie in the mirror planes that intersect the center of the unit cell. The Co–Co distance between adjoining CoN_2 ions on the face is 6.325 Å, and the distance between CoN_2 ions that lie along the face diagonal is 8.945 Å. The closest Co–Co distance (4.613 Å) is between cobalt atoms on the face and in the mirror plane which bisects the unit cell. There are 24 cobalt atoms in the unit cell having a formal mixed valence (18 Co^{I} and 6 Co^{II}), and all of the cobalt atoms reside on crystallographically equivalent sites. Although the condition of mixed valence on equivalent sites should lead to a metallic ground state as described by Robin and Day as a type IIIB conductor (51), local structural distortions due to the disordered Sr1 would make the cobalt positions inequivalent and may lead to localized electrons which possess a magnetic moment (vide infra). Of the nitrogen atoms that are bonded to the cobalt atom, one is octahedrally coordinated (5 Sr, 1 Co; d(Co–N) = 1.79 Å) and the other is in a trigonal prism composed of six strontium atoms and capped by one cobalt atom (d(Co–N) = 1.83 Å) (Fig. 4). The Co–N bond distances are similar to those in $LiSr_2CoN_2$ (d(Co–N) = 1.81 Å) and BaCoN (d(Co–N) = 1.74–1.87 Å). The 7-coordinated nitrogen atom (6 Sr, 1 Co for $Sr_{39}Co_{12}N_{31}$) is also seen in Ca_6GeN_5 and Ca_6FeN_5 (6 Ca, 1M) (52). In addition to the previously mentioned late transition metal nitrides (see Introduction), linearly coordinated moieties are found in d^{10} Cu^{I}, Ag^{I}, and Au^{I} compounds as oxides, sulfides, cyanides, and ammonia complexes. Linear species are also found in the pyrochlore and delafossite structures for several metals (53).

Focusing instead on the strontium–nitrogen network, we present in Fig. 5 all nitrogen-centered polyhedra. This network illustrates the complexity of the $Sr_{39}Co_{12}N_{31}$ structure. To clarify, the Sr–N subframework, which is represented by the lightly colored octahedra, is constructed with two crystallographically equivalent lattices of

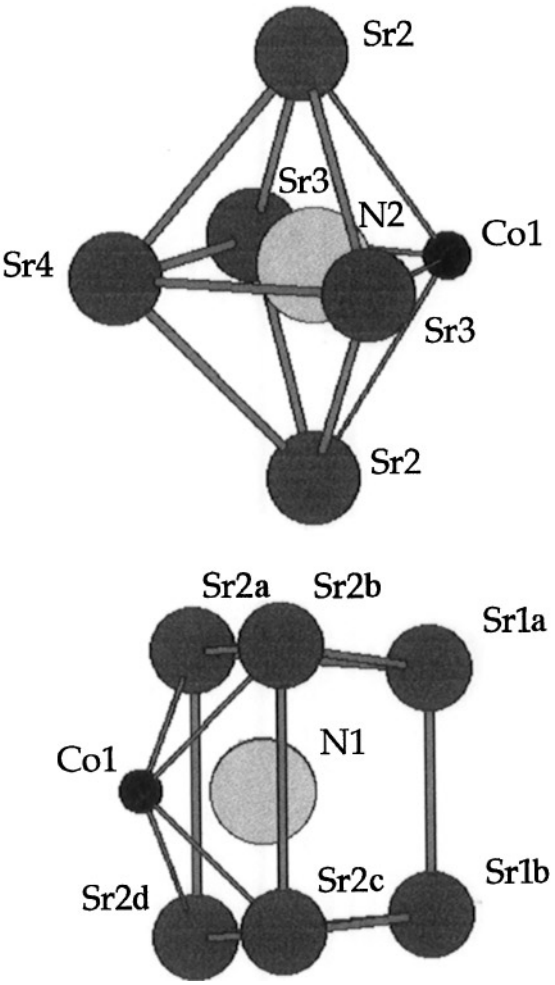

FIG. 4. Coordination polyhedra centered about N2 (top) and N1 (bottom) are illustrated. The atoms are represented as circles of arbitrary size. The N2 position is centered in pseudo-octahedral coordination (5 Sr, 1 Co), and the N1 position lies in a distorted capped trigonal prism (6 Sr, 1 Co). The Sr1 position is located on the high-symmetry site for clarity.

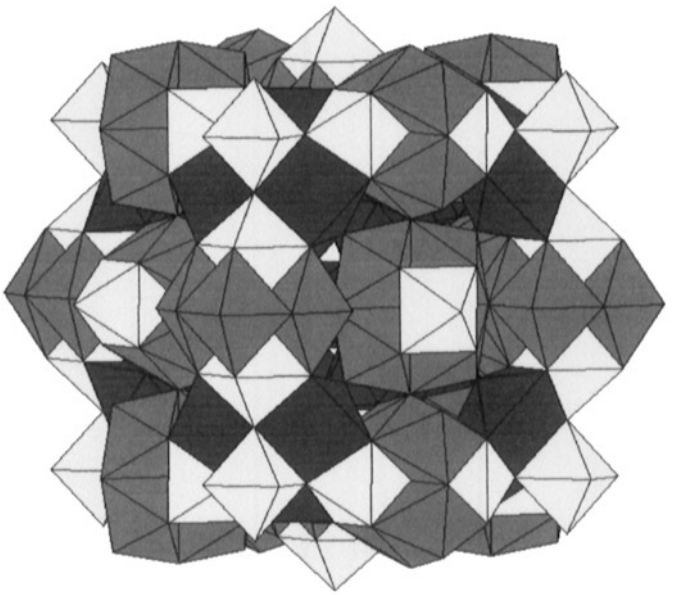

FIG. 5. The Sr–N network presented as nitrogen-centered polyhedra. The light octahedra are centered about N3 and N4, the gray octahedra are about N2, and the dark capped trigonal prisms are about N1. The Sr1 position is located at the high-symmetry site for clarity. Clusters of six edge-sharing octahedra are formed about $(0, \frac{1}{2}, \frac{1}{2})$, and all of the edges of the octahedron centered about N4 are shared by the trigonal prism. Also, the triangular faces of the capped trigonal prism are shared with the adjoining octahedra centered about N3.

interpenetrating, nonintersecting, vertex-sharing, nitrogen-centered octahedra, related by the body-centering symmetry. This subframework is built around two nitrogen atoms, located at (0, 0, 0) and (0.328, 0, 0), which are in octahedral coordination with six surrounding strontium atoms.

The disordered strontium atom, Sr1, is coordinated to the nitrogen atom at the origin. The strontium atoms in the split positions are separated by 0.99 Å into four crystallographically equivalent sites, each having $\frac{1}{4}$ occupancy (Fig. 6). Only one position can be occupied for each local arrangement because the Sr–Sr distance between split sites is much smaller than the distance determined by the ionic radius for strontium ($r = 1.32$ Å for CN = 6), in addition to typical Sr–Sr distances, which are greater than 3.5 Å in nitrides (e.g., the distorted nitrogen-centered octahedron in Sr_2N has Sr–Sr bond distances within 3.52 and 3.86 Å) (34). Further examination of this disorder, specifically, evaluation of the $Sr_{39}Co_{12}N_{31}$ structure in lower symmetry space groups with the same unit cell, did not lead to any solution that would provide an ordered model.

Bond Valence Calculations

Bond valence calculations performed by EUTAX (54) indicate that the atoms in $Sr_{39}Co_{12}N_{31}$ reside in coordination environments similar to those in $LiSr_2CoN_2$ (14) and Sr_2N (34). The results of the calculations are presented in Table 6. For all compounds, the bond valence sum for strontium is slightly lower than the expected atomic valence of 2. Likewise the sum for the nitrogen atoms is less than 3, which is the expected value for a nitride anion. As an exception, the nitrogen valence in $LiSr_2CoN_2$ is slightly greater than 3. However, this is common for lithium-containing nitrides, and it is attributed to enhanced charge transfer (55). The inductive effect leads to short Co–N bond distances, which is observed in a valence sum for cobalt that is substantially higher than anticipated for Co^{I} (56). These factors suggest that the parameters used for the calculation are inappropriate due to the covalent nature of nitrides. In spite of that, this information can be used to determine possible sites for mixed anion or cation occupancies. For

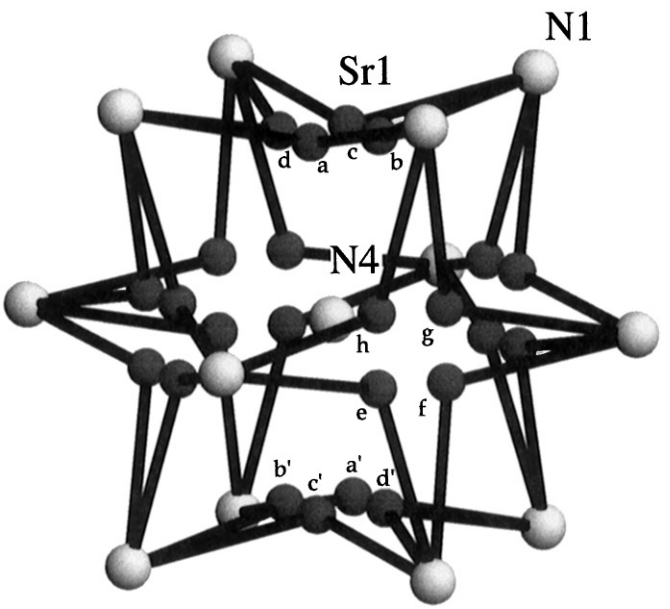

FIG. 6. The disordered Sr1 position is shown in dark gray with nitrogen atoms in light gray. This cluster is a representation of the disordered nitrogen-centered octahedra about (0, 0, 0) and $(\frac{1}{2}, \frac{1}{2}, \frac{1}{2})$. Neither the edge-capping nitrogen atoms nor the central nitrogen position at the origin exhibits disorder.

example, Sr2 has a value very close to 1, which one would expect for an alkali metal, such as sodium. However, attempts to solve the crystal structure with a partial sodium occupation were unsatisfactory. As another example, one might suspect that the N1 or N3 positions may be partially occupied with oxygen, leading to the low valence sum. However, the N4 position would be the most chemically reasonable site for oxygen since it is the only position solely coordinated by strontium, therefore giving it the most electropositive character. Further refinements were unstable when oxygen was placed on any site. Based on these observations, the bond valence sums appear to reflect the open nature of the $Sr_{39}Co_{12}N_{31}$ structure.

TABLE 6
Results from EUTAX Bond Valence Calculations

Compound	Atom	$\sum v_i$
$LiSr_2CoN_2$	Sr	1.452
	Co	2.554
	Li	0.780
	N	3.119
$Sr_{39}Co_{12}N_{31}$	Sr1	1.582
	Sr2	1.094
	Sr3	1.335
	Sr4	1.648
	Co	2.152
	N1	2.387
	N2	2.561
	N3	2.330
	N4	2.526
Sr_2N	Sr	1.224
	N	2.45

Magnetic Susceptibility

Typically, solid-state compounds having isolated anions with late transition metals behave as Mott insulators. However, the late transition metal nitrides lie close to the metal–insulator border. Metallic character has been observed for isolated nitridoniccolate anions in Sr_2NiN_2 (27), whereas in $Sr_{39}Co_{12}N_{31}$, which has isolated nitridocobaltate anions, the electrons in the *d* orbitals are localized and demonstrate antiferromagnetic interactions typical of Mott insulators.

The temperature-dependent data were fit to the Curie–Weiss law. The plot of $1/\chi_g$ (inverse gram susceptibility) versus temperature is shown in Fig. 7. At temperatures above the Neél temperature, a typical antiferromagnet demonstrates a linear relationship of the inverse susceptibility with respect to temperature, intercepting the temperature axis at negative values. The Neél temperature is usually observed as a sharp decrease of the susceptibility (or increase of the inverse susceptibility) and is an indication of an ordering of spins in the antiferromagnet. In the case of $Sr_{39}Co_{12}N_{31}$, an ordering is not observed, but there is a slight decrease in the slope of the inverse susceptibility at 12 K. This behavior has previously been observed in frustrated magnetic systems (57).

For $Sr_{39}Co_{12}N_{31}$, the Curie–Weiss fit over $30 < T < 230$ K yielded the following values: $C_g = 8.21 \times 10^{-3}$ emu g^{-1} K^{-1}, $\chi_0 = 7.94 \times 10^{-7}$ emu g^{-1}, and $\Theta = 74.6$ K. Therefore, the effective magnetic moment per formula unit, $\mu_{eff}(Sr_{39}Co_{12}N_{31})$, is 17.29 μ_B and per cobalt atom, μ_{eff}/Co, is 4.99 μ_B. As mentioned earlier, there is a formal mixed valence of the cobalt, 18 Co^{I} and 6 Co^{II}, per unit cell. The low coordination (2-fold) of the cobalt leads to a weak crystal field; therefore we expect high-spin ground states. The Co^{II} has $S = \frac{3}{2}$, which gives a spin-only magnetic moment of 3.87 μ_B, whereas Co^{I} in linear coordination has $S = 1$ and a spin-only magnetic moment of 2.83 μ_B. The observed value for the effective magnetic moment is greater than the spin-only value, indicating that there is a significant orbital contribution to the magnetic moment, which is common in cobalt compounds due to spin–orbit interactions (58). Due to two distinct valences on cobalt, the magnetic moment can be modeled as

$$\mu_{eff}^2 = [g_1 X_1 S_1(S_1 + 1) + g_2 X_2 S_2(S_2 + 1)]$$

where $X_1 = 0.25$ is the atomic fraction of Co^{II} with $S_1 = \frac{3}{2}$ and $X_2 = 0.75$ is the atomic fraction of Co^{I} with $S_2 = 1$. Since the observed moment per cobalt is $\mu_{eff} = 5$, g would

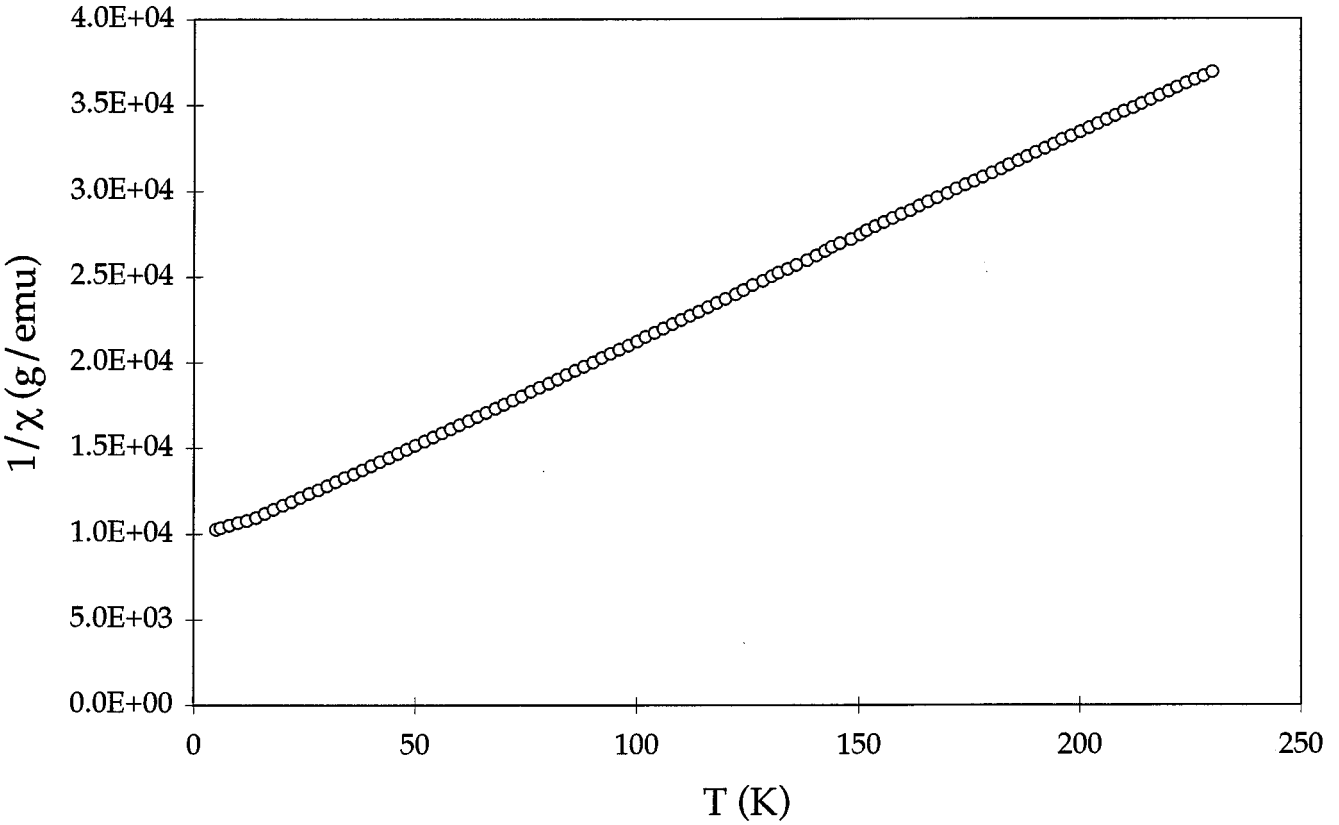

FIG. 7. Magnetic susceptibility of $Sr_{39}Co_{12}N_{31}$ exhibiting antiferromagnetic interactions as shown by the plot of inverse gram susceptibility versus temperature. The observed effective magnetic moment is 4.99 μ_B.

be 3.20, assuming an average value. Many 3*d* elements have a *g* close to 2, but for cobalt *g* is typically higher. Empirical evidence is abundant for unusually high effective magnetic moments on cobalt in other compounds. For high-spin Co^{II} (d^7) in tetrahedral or octahedral coordination, the effective spin-only moment is 3.87 μ_B, but typical observed values are in the range 4.3–5.6 μ_B, (59). For example, the reported magnetic moment for octahedral Co^{II} in $BaCoF_4$ powder is 5.49 μ_B (60). Following a similar analysis as above for the fluoride, *g* equals 2.84.

Only a few examples of linearly coordinated cobalt exist, and fewer have reported magnetic data. Table 7 lists the bond distances and magnetic data for $Sr_{39}Co_{12}N_{31}$; $LiSr_2CoN_2$; bis(bis(diphenylmethylsilyl)amido-*N*)cobalt, $Co\{N(SiMePh_2)_2\}_2$ (61); bis(*N* − (dimesitylboryl)-anilido-*N*)cobalt, $Co(NPhBMes_2)_2$ (62); and bis(*N* − (dimesitylboryl)-(*N*-(mesitylamino)-anilido-*N*)cobalt, $Co(NMesBMes_2)_2$ (62). For the molecular compounds, longer Co–N bond distances decrease the overlap of atomic orbitals. In addition, the distortions from a 180° bond angle remove orbital degeneracies which tend to quench the orbital angular momentum. These conditions may explain why the observed magnetic moments for the molecular species are near the spin-only value with *g* close to 2. More data are necessary to elucidate the magnetic behavior of linearly coordinated compounds.

In conclusion, the reaction of strontium, cobalt, and sodium azide in a liquid sodium flux yields an unusual $Sr_{39}Co_{12}N_{31}$ phase with a unique structure type in cubic $Im\bar{3}m$ symmetry. The cobalt is located in linear coordination as isolated nitridometalate ions having a formal mixed valence of Co^{I} and Co^{II}. The magnetic susceptibility demonstrates antiferromagnetic Curie–Weiss behavior.

TABLE 7
Magnetic Data of Linearly Coordinated Cobalt Compounds

Compound	N–Co–N bond angle (deg)	Co–N bond distance (Å)	$\mu_{eff}/Co\mu_B$	*g*
$Sr_{39}Co^{I/II}_{12}N_{31}$	180	1.79, 1.83	4.99	
$LiSr_2Co^{I}N_2$	180	1.81		
$Co^{II}\{N(SiMePh_2)_2\}_2$	147.0	1.898, 1.904		
$Co^{II}(NPhBMes_2)_2$	127.1	1.909 av	4.11[a]	2.11[b]
$Co^{II}(NMesBMes_2)_2$	168.4	1.910 av	4.36[a]	2.10[b]

[a]The magnetic moment was determined in C_6H_6/C_6D_6 solution via the Evans method. D. F. Evans, *J. Chem. Soc., Dalton Trans.* 2005 (1959).

[b]The ESR spectra were measured on crystalline samples between 7.5 and 11 K with a typical scan range of $(3–5) \times 10^3$ G.

ACKNOWLEDGMENTS

The authors are grateful for the use of the diffractometer and SQUID at the NEC Research Institute in Princeton, NJ. We also thank Robert C. Haushalter and Christopher D. W. Jones for helpful discussions. The research at Cornell University was funded by the National Science Foundation.

REFERENCES

1. F. J. DiSalvo and S. J. Clarke, *Curr. Opin. Solid State Mater. Sci.* **1,** 241 (1996).
2. G. A. Slack, R. A. Tanzilli, R. O. Pohl, and J. W. Vandersande, *J. Phys. Chem. Solids* **48,** 641 (1987).
3. C. K. Narula, J. E. Allison, D. R. Bauer, and H. S. Gandhi, *Chem. Mater.* **8,** 984 (1996).
4. A. Münster, *Angew. Chem.* **69,** 281 (1957).
5. S. Nakamura, T. Mukai, and M. Senoh, *Appl. Phys. Lett.* **64,** 1687 (1994).
6. T. H. Geballe, B. T. Matthias, J. P. Remeika, A. M. Clogston, V. B. Compton, J. P. Maita, and H. J. Williams, *Physics* **2,** 293 (1996).
7. A Gudat, *Dissertation*, Universität Düsseldorf, 1990.
8. W. Sachsze and R. Juza, *Z. Anorg. Allg. Chem.* **259,** 278 (1949).
9. A. Gudat, R. Kniep, and A. Rabenau, *Thermochim. Acta* **160,** 49 (1990).
10. A. Gudat, R. Kniep, and A. Rabenau, *Angew. Chem., Int. Ed. Engl.* **30,** 199 (1991).
11. A. Gudat, R. Kniep, and A. Rabenau, *Z. Anorg. Allg. Chem.* **607,** 8 (1992).
12. J. Jaeger and R. Kniep, *Z. Naturforsch, B* **47,** 1290 (1992).
13. G. Cordier, A. Gudat, R. Kniep, and A. Rabenau, *Angew. Chem., Int. Ed. Engl.* **28,** 1702 (1989).
14. P. Höhn and R. Kniep, *Z. Naturforsch, B* **47,** 434 (1992).
15. M. Y. Chern and F. J. DiSalvo, *J. Solid State Chem.* **88,** 459 (1990).
16. A. Gudat, R. Kniep, and J. Maier, *J. Alloys Compd.* **186,** 339 (1992).
17. T. Yamamoto, S. Kikkawa, and F. Kanamaru, *J. Solid State Chem.* **115,** 353 (1995).
18. A. Gudat and R. Kniep, *J. Alloys Compd.* **179,** 333 (1992).
19. A. Gudat, S. Haag, R. Kniep, and A. Rabenau, *J. Less-Common Met.* **159,** L29 (1990).
20. J. Jaeger, *Dissertation*, TH Darmstadt, 1995.
21. A. Tennstedt and R. Kniep, *Z. Anorg. Allg. Chem.* **620,** 1781 (1994).
22. U. Zachwieja and H. Jacobs, *Eur. J. Solid State Inorg. Chem.* **28,** 1055 (1991).
23. R. J. Arnott and A. Wold, *J. Phys. Chem. Solids* **15,** 152 (1960).
24. P. Höhn and R. Kniep, *Z. Naturforsch, B* **47,** 477 (1992).
25. A. Gudat, W. Milius, S. Haag, R. Kniep, and A. Rabenau, *J. Less-Common Met.* **168,** 305 (1991).
26. A. Gudat, R. Kniep, and A. Rabenau, *Z. Anorg. Allg. Chem.* **597,** 61 (1991).
27. G. R. Kowach and F. J. DiSalvo, unpublished data.
28. F. J. DiSalvo, S. S. Trail, H. Yamane, and N. E. Brese, *J. Alloys Compd.* **255,** 122 (1997).
29. M. Y. Chern and F. J. DiSalvo, *J. Solid State Chem.* **88,** 528 (1990).
30. H. Yamane and F. J. DiSalvo, *J. Solid State Chem.* **119,** 375 (1995).
31. T. Yamamoto, S. Kikkawa, and F. Kanamaru, *J. Solid State Chem.* **119,** 161 (1995).
32. A. L. Wayda and J. L. Dye, *J. Chem. Educ.* **62,** 356 (1985).
33. W. E. Ford, *in* "Dana's Textbook of Mineralogy," 4th ed., p. 75. John Wiley & Sons, New York, 1932.
34. N. E. Brese and M. O'Keeffe, *J. Solid State Chem.* **87,** 134 (1990).
35. Microprobe data: 100-s scans were taken on a Hitachi scanning electron microscope (SEM) equipped with a Princeton Gamma Tech energy-dispersive spectrometer (EDS).
36. F. Hai-Fu, Structure Analysis Programs with Intelligent Control, Rigaku Corp. 1990.
37. Crystal Structure Analysis Package, Molecular Structure Corp., 1985, 1992.
38. G. R. Kowach, unpublished results.
39. R. Niewa and H. Jacobs, *Chem. Rev.* **96,** 2053 (1996).
40. E. Veleckis, K. E. Anderson, F. A. Cafasso, and H. M. Feder, *in* "Proceedings of the International Conference on Sodium Technology and Fast Reactor Design," Part I, ANL-7520, p. 295. Argonne National Laboratory, Argonne, IL, 1968. (E. Veleckis, K. E. Anderson, F. A. Cafasso, and H. M. Feder, *Nucl. Sci. Abstr.* **23,** 45237 (1969)).
41. C. C. Addison, R. J. Pulham, and E. A. Trevillion, *J. Chem. Soc., Dalton Trans.* 2082 (1975), and references therein.
42. R. Thompson, *J. Inorg. Nucl. Chem.* **34,** 2513 (1972).
43. C. C. Addison, G. K. Creffield, P. Hubberstey, and R. J. Pulham, *J. Chem. Soc., Dalton Trans.* 1105 (1976).
44. P. E. Rauch and A. Simon, *Angew. Chem., Int. Ed. Engl.* **31,** 1519 (1992).
45. G. J. Snyder and A. Simon, *J. Am. Chem., Soc.* **117,** 1996 (1995).
46. G. J. Snyder and A. Simon, *Angew. Chem., Int. Ed. Engl.* **33,** 689 (1994).
47. U. Steinbrenner and A. Simon, *Angew. Chem., Int. Ed. Engl.* **35,** 552 (1996).
48. A. Simon and U. Steinbrenner, *J. Chem. Soc., Faraday Trans.* **92,** 2117 (1996).
49. R. L. Eichelberger and R. L. McKisson, *Nucl. Sci. Abstr.* **24,** 36891 (1970).
50. T. A. Kovacina and R. R. Miller, U.S. *Govt. Res. Dev. Rep.* **69,** 71 (1969).
51. M. B. Robin and P. Day, *in* "Advances in Inorganic Chemistry and Radiochemistry," Vol. 10, p. 247. Academic Press, New York, 1967.
52. G. Cordier, P. Höhn, R. Kniep, and A. Rabenau, *Z. Anorg. Allg. Chem.* **591,** 58 (1990).
53. A. F. Wells, *in* "Structural Inorganic Chemistry," 5th ed., p. 1103. Oxford University Press, New York, 1991.
54. N. E. Brese and M. O'Keeffe, *Acta Crystallogr., Sect. B* **47,** 192 (1991).
55. N. E. Brese, *Struct. Bonding* **79,** 307 (1992).
56. J. Etourneau, J. Portier, and F. Menil, *J. Alloys Compd.* **188,** 1 (1992).
57. A. Ramirez, *Annu. Rev. Mater. Sci.* **24,** 453 (1994).
58. C. J. O'Connor, *Prog. Inorg. Chem.* **29,** 203 (1982).
59. A. F. Wells, *in* "Structural Inorganic Chemistry," 5th ed., p. 1209. Oxford University Press, New York, 1991.
60. A. Chrétien, and M. Samouël *Monatsh. Chem.* **103,** 17 (1972).
61. R. A. Bartlett and P. P. Power, *J. Am. Chem. Soc.* **109,** 7563 (1987).
62. H. Chen, R. A. Bartlett, M. M. Olmstead, P. P. Power, and S. C. Shoner, *J. Am. Chem. Soc.* **112,** 1048 (1990).